boundary-layer thickness $\delta_2/d = 0.003$, the c_{pB} values should also be constant for each Mach number. One can see that this nearly is the case. The deviations from a mean value in each group are relatively small. At $M_\infty \approx 2.85$, the deviations depend partly on the fact that the Mach number is not constant, but varies from $M_\infty = 2.81$ at $\delta_2/d = 0.19$ to $M_\infty = 2.89$ at $\delta_2/d = 0.70$.

There are, of course, several other theories for prediction of the base pressure in two-dimensional supersonic flow. Perhaps the most important are based on the flow model of Chapman[6] and Korst[7] where the basic physical idea is that the base pressure can be predicted if the pressure at the reattachment point (see Fig. 1) is known. Of these theories, we additionally mention only those of Refs. 8-10, which allow the prediction of the influence of the boundary-layer thickness on the base pressure. The theories have been discussed and compared in Ref. 11. It seems that the theory of McDonald[10] agrees at least qualitatively with experiment, whereas Refs. 8 and 9 overestimate the effect of the boundary-layer thickness. Experimental results exist obviously only for $\delta_2/d \leq 0.10$.

References

[1]Tanner, M., "Theoretische Bestimmung des Basisdruckes für zwei-dimensionale turbulente Totwasserströmungen bei Überschallgeschwindigkeiten," DFVLR-FB 80-19, 1980.

[2]Tanner, M., "Steady Base Flows," *Progress of Aerospace Sciences*, Vol. 21, No. 2, 1984, pp. 81-157.

[3]Goecke, S., "Flight-Measured Pressure Characteristics of Aft-Facing Steps in High Reynolds Number Flow at Mach Numbers of 2.20, 2.50 and 2.80 and Comparison with Other Data," NASA TM-72855, 1978.

[4]Oswatitsch, K., "Der Luftwiderstand als Integral des Entropiestromes," *Nachrichten der Akademie der Wissenschaften in Göttingen, Mathematisch-Physikalische Klasse*, 1945, pp. 88-90.

[5]Oswatitsch, K., *Grundlagen der Gasdynamik*, Springer Verlag, New York, 1976.

[6]Chapman, D. R., Kuehn, D. M., and Larson, H. K., "Investigation of Separated Flows in Supersonic and Subsonic Streams with Emphasis on the Effect of Transition," NACA Rept. 1356, 1958.

[7]Korst, H. H., "A Theory for Base Pressures in Transonic and Supersonic Flow," *Journal of Applied Mechanics*, Vol. 23, 1956, pp. 593-600.

[8]Nash, J. F., "An Analysis of Two-Dimensional Turbulent Base Flow, Including the Effect of the Approaching Boundary Layer," British Aeronautical Research Council, R&M 3344, 1963.

[9]Roberts, J. B., "On the Prediction of Base Pressure in Two-Dimensional Supersonic Turbulent Flow," British Aeronautical Research Council, R&M 3434, 1966.

[10]McDonald, H., "The Turbulent Supersonic Base Pressure Problem: A Comparison Between a Theory and Some Experimental Evidence," *The Aeronautical Quarterly*, Vol. 17, 1966, pp. 105-126.

[11]Tanner, M., "Theoretical Prediction of Base Pressure for Steady Base Flow," *Progress of Aerospace Sciences*, Vol. 14, 1973, pp. 177-225.

Block-Implicit Calculations of Three-Dimensional Laminar Flow in Strongly Curved Ducts

S. Pratap Vanka*

Argonne National Laboratory, Argonne, Illinois

Nomenclature

A_p, A_i = coefficients in the finite difference equation
d = width (and height) of the duct
p = pressure
r, θ, z = coordinate distances
$\bar{S}$ = integrated source term
v_b = bulk axial velocity
v_r, v_θ, v_z = linear velocities in r, θ, and z directions, respectively
x = distance in the straight sections
ρ = fluid density
μ = fluid viscosity

Received April 11, 1984; revision received Jan. 16, 1985. This paper is declared a work of the U.S. Government and therefore is in the public domain.

*Engineer, Components Technology Division. Member AIAA.

Introduction

THE understanding of flow development in ducts with longitudinal curvature is of interest in the design of aircraft intakes, turbomachinery passages, and heat exchange equipment. A number of previous studies[1-5] have attempted to solve numerically the partial differential equations appropriate to the curved duct configuration. Experimental studies quantifying the velocity and pressure fields also have been made.[4,6,7] A review of flow development in curved circular pipes was recently made by Berger et al.[8]

This Note describes the numerical solution of the elliptic partial differential equations governing three-dimensional fluid flow in strongly curved rectangular ducts by the use of a fully coupled block-implicit solution algorithm. Calculations have been made for the configuration of Humphrey et al.[4] It is observed that the coupled solution of the momentum and continuity equations converges rapidly and reduces the required computing time by a factor of 2.5 over a decoupled solution such as that by Humphrey et al.[4] The flowfield calculated here is in good agreement with the experimental data and with previous calculations.[4] The flow separation on the outer sidewall is well predicted, in conformity with earlier observations.

Equations Solved

Theoretical studies of curved duct flow development need the solution of complete elliptic Navier-Stokes equations governing steady three-dimensional flows. At small curvatures, however, the flow may be considered parabolic[9] or partially parabolic[10] and streamwise diffusion may be neglected. The present study is concerned with the calculation of flow in strongly curved ducts with regions of axial flow reversal. Consequently, the following three-dimensional elliptic equations are solved.

$$\rho\left(v_r\frac{\partial v_r}{\partial r}+\frac{v_\theta}{r}\frac{\partial v_r}{\partial \theta}+v_z\frac{\partial v_r}{\partial z}-\frac{v_\theta^2}{r}\right) = -\frac{\partial p}{\partial r}+\mu\left(\nabla^2 v_r-\frac{v_r}{r^2}-\frac{2}{r^2}\frac{\partial v_\theta}{\partial \theta}\right) \quad (1)$$

$$\rho\left(v_r\frac{\partial v_\theta}{\partial r}+\frac{v_\theta}{r}\frac{\partial v_\theta}{\partial \theta}+v_z\frac{\partial v_\theta}{\partial z}+\frac{v_r v_\theta}{r}\right) = \frac{1}{r}\frac{\partial p}{\partial \theta}+\mu\left(\nabla^2 v_\theta+\frac{2}{r^2}\frac{\partial v_r}{\partial \theta}-\frac{v_\theta}{r^2}\right) \quad (2)$$

$$\rho\left(v_r\frac{\partial v_z}{\partial r}+\frac{v_\theta}{r}\frac{\partial v_z}{\partial \theta}+v_z\frac{\partial v_z}{\partial z}\right) = -\frac{\partial p}{\partial z}+\mu\nabla^2 v_z \quad (3)$$

$$\frac{\partial v_z}{\partial r}+\frac{1}{r}\frac{\partial v_\theta}{\partial \theta}+\frac{\partial v_z}{\partial z}+\frac{v_r}{r}=0 \quad (4)$$

and

$$\nabla^2 = \frac{\partial^2}{\partial r^2}+\frac{1}{r^2}\frac{\partial^2}{\partial \theta^2}+\frac{\partial^2}{\partial z^2}+\frac{1}{r}\frac{\partial}{\partial r}$$

The above equations are solved with boundary conditions appropriate to the experimental configuration.

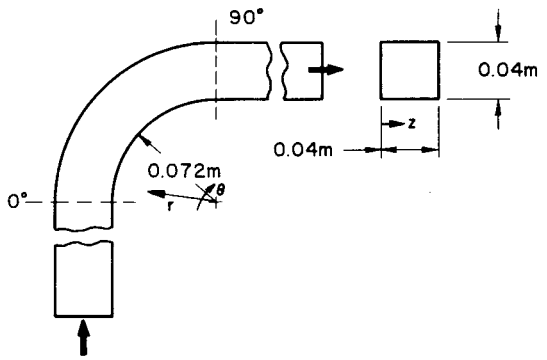

Fig. 1 Duct configuration and coordinate system.

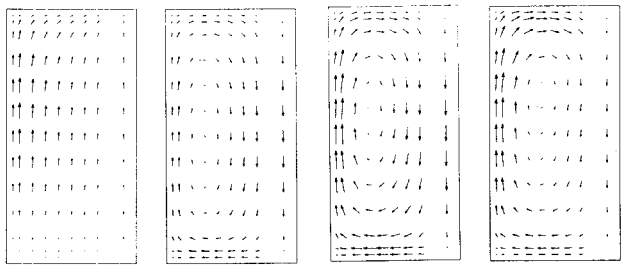

Fig. 2 Secondary flow patterns at a) $x=-0.1\ d$; b) $\theta=15$ deg; c) $\theta=30$ deg; d) $\theta=60$ deg.

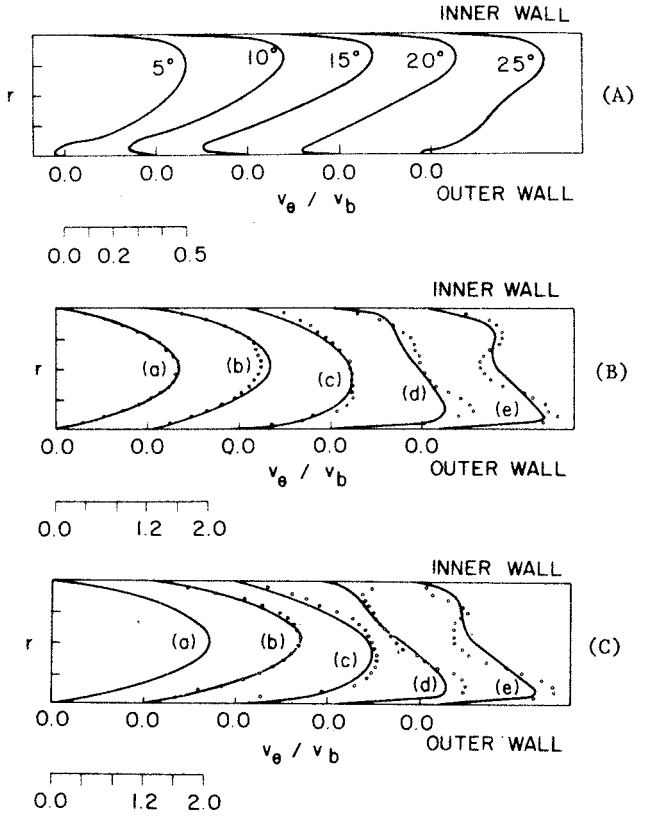

Fig. 3 Development of axial velocity at A) 1mm, B) 10 mm, and C) 20 mm from bottom wall: -- predictions, o data (Ref. 4) at (a) $x=-5\ d$, (b) $\theta=0$ deg, (c) $\theta=30$ deg, (d) $\theta=60$ deg, (e) $\theta=90$ deg.

Solution Algorithm

Finite Differencing

The discrete equations are derived by integrating the governing equations over "control volumes." A staggered mesh system is used in locating the velocities and pressure. The momentum equations are integrated over subregions surrounding the location of the velocity. The practices used in the integration process are similar to those of Pratap and Spalding.[10] However, a difference in current practice is the use of exponential functions for the internode variation of the variables.

After the integration of individual convective and diffusive fluxes in the r, z, and θ directions and the source terms, the equations can be concisely written in the form

$$A_P\phi_P=\Sigma A_i\phi_i+\bar{S} \tag{5}$$

where ϕ is any one of the three velocities. The A link the neighboring values of ϕ with the variable being solved for. The term $\bar{S}$ is the integrated value of the "source term" in the equations (those not represented by the standard divergence form). The continuity equation is integrated by summing the mass fluxes in and out of the control volumes surrounding the grid nodes.

Solution of Equations

The present solution procedure is based on recognition of the strong interaction between the pressure and velocity fields. The set of nonlinear equations are therefore solved by a block-implicit method. The equations are first grouped at each node and the blocks are then combined into one large set. Symbolically, we seek the solution to

$$F(X)=0$$

where

$$X_{ijk}=(v_\theta,v_r,v_z,p)^T_{ijk}$$

$$F_{ijk}=(F_\theta,F_r,F_z,F_c)^T_{ijk} \tag{6}$$

and where the column vector X denotes the blocked set of unknown velocities and pressures and F the finite difference equation set. This large set of nonlinear equations may be solved through a Newton or Newton-Raphson method combined with direct or iterative inversion of the linear equations. However, because of the unsymmetric nature of the equations, iterative solutions of the linear equations are unreliable and may be slow to converge for the present system. Also, the use of a direct solution of three-dimensional equations through Gaussian elimination is not practical for large systems.

These constraints on the available computer memory and the need for reliability have led us to employ a plane-by-plane solution of the equations. The plane-by-plane solution enjoys the benefit of rapid transfer of information along the direction perpendicular to the planes and, if this is chosen properly, can lead to rapid convergence. In the curved duct case, except in the regions of negative axial velocity, the axial θ direction is the most suitable one for such plane-by-plane sweeps. Therefore, the present algorithm solves the blocked nonlinear equations on successive (r-z) planes. At each plane, the velocities v_r and v_z located in the plane and the v_θ velocities in front of the plane (note the staggered mesh arrangement) are solved.

First, the nonlinear equations are linearized with the values currently in the computer storage. The two-dimensional set of linear equations is then solved by an efficient sparse Gaussian elimination routine.[11] For the sake of reliability, a direct inversion routine is currently preferred over an iterative algorithm. The linear equations are solved for the corrections by first calculating the residuals in the equations. The corrections are applied to the existing fields of velocity and pressure. The flow domain is repeatedly swept with the plane-by-plane solution until the residuals have decreased to small values. The CPU time required by the direct inversion process is reduced through preordering the blocks of equations on alternate

diagonals and by calculating the LU factorizations of the coefficient matrices only at selected cross-sectional planes (this is similar to a Newton's chord method). A small amount of under-relaxation was found necessary on the corrections made to the velocities and pressures.

Results

Calculations have been made for the experimental configuration of Humphrey et al.[4] The coordinate system is shown in Fig. 1. The duct is of square cross section ($d = 0.04$ m) and has a radius of curvature of 0.072 m. The curved duct is preceded and followed by straight sections. The Reynolds number of the flow based on the duct width and the inlet bulk velocity v_b is 792.0. The flow is considered fully developed at a station 0.2 m (5 d) upstream of the 0 deg of the bend. The present calculations were made with a $(58 \times 15 \times 11)$ (θ,r,z) grid that is nearly the same size as that used by Humphrey et al. $(60 \times 15 \times 10)$. Because of symmetry conditions, only half of the duct was solved.

Fully developed duct flow profiles were first generated by solving the equations of a straight duct. These were then prescribed at the inlet plane. A zero derivative exit boundary condition was prescribed at $x = 10\ d$ in the aft straight duct. The calculations were started with simplistic guesses to the velocity and pressure fields. The normalized maximum residuals in the momentum and continuity equations are monitored with iteration number. The present calculations converge rapidly to residuals of 10^{-3} in about 40 iterations. The CPU time on an IBM 3033 was 8 min, which reflects a factor of 2.5 improvement over the time quoted by Humphrey et al. (after considering the relative speeds of the computers involved). Additional computational efficiencies can be gained by developing a reliable iterative algorithm in place of the direct inversion procedure.

Figure 2 shows the calculated secondary flow patterns at four axial locations. It can be seen that the secondary flow is already present upstream of the 0 deg station as a consequence of the ellipticity in the flow. The secondary velocities increase in magnitude with bend angle, reaching a value in excess of 50% of the bulk velocity in regions close to the bottom wall.

Figure 3 shows the development of the axial velocity at different heights from the bottom wall. It is observed that in the initial region of the bend the flow has separated from the outer sidewall at $z = 1$ mm as a consequence of the large adverse pressure gradient. The development of the axial velocity profiles agrees satisfactorily with the experimental data and calculations of Humphrey et al. Further improvement in the agreement is possible, however, through the use of more grid nodes in regions of large-velocity gradients.

References

[1]Pratap, V. S. and Spalding, D. B., "Numerical Computations of the Flow in Curved Ducts," *The Aeronautical Quarterly*, Vol. 26, Pt. 3, Aug. 1975, pp. 219-228.

[2]Ghia, K. N. and Sokhey, J. S., "Laminar Incompressible Viscous Flow in Curved Ducts of Regular Cross Sections," *Transactions of ASME, Journal of Fluids Engineering*, Vol. 99, Dec. 1977, pp. 640-648.

[3]Joseph, B., Smith, E. P., and Adler, R. J., "Numerical Treatment of Laminar Flow in Helically Coiled Tubes of Square Cross Section," *AIChE Journal*, Vol. 21, No. 5, Sept. 1975, pp. 965-974.

[4]Humphrey, J. A. C., Taylor, A. M. K., and Whitelaw, J. H., "Laminar Flow in a Square Duct of Strong Curvature," *Journal of Fluid Mechanics*, Vol. 83, Pt. 3, 1977, pp. 509-527.

[5]Mori, Y., Uchida, Y., and Ukon, J., "Forced Convective Heat Transfer in a Curved Channel with a Square Cross Section," *International Journal of Heat and Mass Transfer*, Vol. 14, 1971, pp. 1787-1805.

[6]Pratap, V. S., "Flow and Heat Transfer in Curved Ducts," Ph.D. Thesis, University of London, London, 1975.

[7]Rowe, M., "Measurements and Computations of Flow in Pipe Bends," *Journal of Fluid Mechanics*, Vol. 43, 1970, pp. 771-783.

[8]Berger, S. A., Talbot, L., and Yao, L-S., "Flow in Curved Pipes," *Annual Review of Fluid Mechanics*, Vol. 15, 1983, pp. 461-512.

[9]Patankar, S. V. and Spalding, D. B., "A Calculation Procedure for Heat, Mass, and Momentum Transfer in Three-dimensional Parabolic Flows," *International Journal of Heat and Mass Transfer*, Vol. 15, 1972, pp. 1787-1806.

[10]Pratap, V. S. and Spalding, D. B., "Fluid Flow and Heat Transfer in Three-dimensional Duct Flows," *International Journal of Heat and Mass Transfer*, Vol. 19, 1976, pp. 1183-1193.

[11]Eisenstat, S. C., Gursky, M. C., Schultz, M. H., and Sherman, A. H., "Yale Sparse Matrix Package: The Nonsymmetric Codes," Yale University, New Haven, CT, Res. Rept. 114, 1975.

Unsteady Transport Effects on Diffusion Flame Stability

T. S. Sheshadri*

Indian Institute of Science, Bangalore, India

Nomenclature

a_1,a_2,a_3,a_4,
b_1,b_2,b_3,b_4 = complex constants
c_1,c_2 = complex constants having "nontransport" and "transport" properties, respectively
L_1,L_2 = complex constants

Remaining nomenclature is identical to that of Ref. 1.

Introduction

ANALYTICAL studies of steady-state diffusion flames are generally based on the Burke-Schumann formulation.[2] If the Burke-Schumann geometry is slightly modified to permit fuel/oxidizer flows up to large radial distances, the resulting diffusion flames induce a steady-state velocity profile that tends to be constant near the axis (because of axisymmetry) and at large radial distances (because of the diminishing effect of the diffusion flames). In order to study the dynamic stability of these flames, it is necessary to generalize the formulation to the unsteady case and to carry out a classical linearized stability analysis, taking care to handle correctly the conditions[3] at the unsteady flame. Such an analysis leads to an eigenvalue differential equation whose solution for the eigenvalue yields the growth (or decay) rate of the disturbances along with their frequency. In such analyses, it is usual, as a first approximation, to neglect unsteady transport effects as these give rise to higher-order derivative terms in the stability formulation. Such simplification generally results in some loss of information concerning the stability problem and the resulting mathematical formulation can be referred to as a simplified eigenvalue problem. In the context of the Burke-Schumann problem, the unsteady transport effects refer to unsteady mass and energy diffusion and unsteady energy conduction. Neglecting these effects corresponds to the formal limit Peclet number $P_c \to \infty$.

An analysis along these lines can be found in Ref. 1, whose problem geometry and linearized unsteady equations constitute a convenient starting point for the present work. In the above analysis, the loss of information referred to earlier manifests itself as an inability of the problem formulation to distinguish between self-excited and damped disturbances. Mathematically, the eigenvalue differential

Received Aug. 14, 1984; revision received Jan. 2, 1985.

*Lecturer, Department of Aerospace Engineering.